

1 This document is the accepted manuscript version of the following article:
2
3 Authors: G. Greco, N. Pugno.
4 Title: How spiders hunt heavy prey: the tangle web as a pulley and spider's lifting mechanics observed and quantified in the
5 laboratory.
6 Journal: JOURNAL OF THE ROYAL SOCIETY INTERFACE
7 Year: 2021
8 Accepted date: 12 January 2020
9 DOI: 10.1098/rsif.2020.0907
10 This manuscript version is made available under the CC-BY-NC-ND 4.0 license Originally uploaded to URL:
11 http://pugno.dicam.unitn.it/NP_PDF/PostPrint/2021-493-Greco.pdf on /16/04/2021

12 How spiders hunt heavy prey: the tangle web as a pulley and spider's lifting
13 mechanics observed and quantified in the laboratory

14 Gabriele Greco¹, Nicola M. Pugno^{1,2*}

15 ¹ Laboratory of Bio-inspired, Bionic, Nano, Meta Materials & Mechanics, Department of Civil,
16 Environmental and Mechanical Engineering, University of Trento, Via Mesiano, 77, 38123 Trento,
17 Italy

18 ² Queen Mary University of London, London, United Kingdom, Mile End Rd, London E1 4NS,
19 United Kingdom

20

21 *Corresponding author: nicola.pugno@unitn.it

22 Keywords: spider silk, Theridiidae, biomechanics, mechanical properties, spider's behaviour

23

24 **Abstract**

25 The spiders of the Theridiidae's family display a peculiar behaviour when they hunt extremely large
26 prey. They lift the quarry, making it unable to escape, by attaching pre-tensioned silk threads to it.
27 In this work, we analysed for the first time in the laboratory the lifting hunting mechanism and, in
28 order to quantify the phenomenon, we applied the lifting mechanics theory. The comparison
29 between the experiments and the theory suggests that, during the process, spider does not stretch
30 the silk too much by keeping it in the linear elastic regime. We thus report here further evidence
31 for the strong role of silk in spiders' evolution, especially how spiders can stretch and use it as an
32 external tool to overcome their muscles' limits and capture prey with large mass.

33

34 **Introduction**

35 Spiders exhibit a large variety of behaviours(1) and, in this context, the ability to use silks has evolved
36 over almost 400 million years to fulfil various functions(2) such as building webs(3) or cocoons(4),
37 for courtship or ballooning(5). For these reasons most spider silks have high tensile strength,
38 extensibility and toughness(6,7), as well as a strong stiffening at high deformations, which has
39 recently been observed by Brillouin light scattering experiments(8,9). Among all the functions that
40 are achieved through silk, the prey capture with webs has always intrigued scientists. As an
41 example, the efficiency of orb webs in stopping flying prey requires high mechanical performances
42 of the webs, which both absorb kinetic energy(10) and minimize the damage after impacts(9).
43 Interestingly, spider silks and webs can also act as external power amplifiers because of the elastic
44 energy stored in the material and the structure. For example, the spider *Hyptiotes cavatus* stretches
45 its web by tightening an anchor line over multiple cycles of limb motion, and then releases its hold
46 on the anchor line when an insect strikes the web, which rapidly tangles it(11). This is a quite rare
47 feature in animals that commonly store the elastic energy in the organisms' own anatomical

48 structures(12–18). Another example of external power amplification could be given by the
49 fascinating hunting behaviours of theridiid spiders(Figure 1a). These spiders use the particular
50 structure of the cobweb, which has gumfoot threads that run from the substrate to the main frame
51 (19). These threads are easily detached from the substrate when disturbed by walking prey and thus
52 release the elastic energy stored in the main frame of the web(20). Consequently, if the prey is small
53 (e.g. ant(21)), the gumfoot threads yank it upwards. In this way, small animals become suspended
54 helplessly in the air. With the increase of the prey dimension, it may happen that more than one
55 single gumfoot thread is involved in the suspension. More commonly, bigger sized preys are not
56 completely lifted by a single thread, and theridiid spiders usually rush down and immobilize such
57 prey using aciniform (wrapping) silk. In both these cases (likely the majority of hunt events in nature)
58 spiders carry the prey back to the retreat on their spinnerets, as seen in practically all web spiders.
59 On the other hand, if the prey is extremely large compared to the spiders (Figure 1b), it poses to it
60 extreme conditions (with a large nutritional reward), and a different hunting behaviour, involving
61 the investigated lifting mechanism, is displayed.

62 Once the large walking prey is attached to a capture sticky thread(22,23) of the 3-dimensional cob
63 web (Figure 1c), the spider lifts it through sequential addition of pre-stretched silk threads produced
64 by major ampullate gland(24) (Figure 1d-f). Between the addition of two threads, the aciniform silk
65 as well as the venom is also used to further immobilize the prey. Again, the lifting prevents prey
66 from escaping their web since it can no longer hold on to the underlying surface. Several records
67 show that small reptiles and mammals are occasionally captured in this way (25,26). The first
68 records published were the cases of a snake (about 55 gr) and a mouse that were not able to move
69 and escape because they were lifted off the ground(27). Interestingly, during prey capture those
70 spiders were continuously moving upward and downward with respect to the prey. This one was
71 gradually lifted to a certain height (more than 10 cm). A subsequent more accurate description
72 revealed that the spider attached to the animal silk threads and their length gradually decreased
73 while the mouse was lifted(24). Mc Keown(28) associated this mechanism to the one used by other
74 spiders (such as *Cyrtophora sp.*, *Olios sp.*, and *Phonognatha sp.*) to lift inanimate objects, e. g. leaves
75 or empty shells that are typically used as a temporary den(29–32). Decary(33) observed that this
76 lifting mechanism allows spiders of the genus *Olios sp.*(34) to lift snail shells that are more than 35
77 times the mass of the animal. As in theridiid spiders, *Olios coenobita* attaches silk threads, gradually
78 shorter in length, to the object to apply a sum of tensions used to counteract gravity. Fage(34)
79 suggested that the lifting of small stones in orb webs was due to the elastic silk threads, and not

80 done by the muscle power of the spider. The spider lifting (and dragging) mechanics was
81 theoretically described by Pugno(35) who also showed how the natural (e.g. nonlinear) behaviour
82 of the spider silk improves the efficiency of the lifting.

83 In this work, we studied experimentally for the first time the lifting mechanics used to hunt
84 extremely large prey displayed by spiders of the family Theridiidae. To explain the phenomenon, we
85 compared the experiments with the predictions of the theoretical model (here adapted)(35). The
86 results are another strong example of the efficiency of the spiders in using silk and their web as
87 external tools (i.e. like a pulley) that make them able to perform actions that would be impossible
88 simply by using their muscles. Moreover, with the support of the mechanical model, we find that
89 spiders apparently do not overstretch the silk threads used in the hunt. The lifting mechanism is,
90 thus, another good example of the central role of silk in spider's evolution.

91

92 **Material and Methods**

93 **The mechanical model**

94 In order to rationalize the lifting observations, we apply the lifting mechanics theory developed by
95 Pugno(35) (for the equations we refer to Figure 2).

96 At each step, the spider adds a thread, with a cross section area A , and the prey moves (if it does)
97 till an equilibrium position. The vertical equilibrium is achieved through the sum of the vertical
98 components of the threads' tensions that balance the weight of the prey. The horizontal equilibrium
99 is achieved through the sum of the horizontal's components of the threads' tensions. For the sake
100 of simplicity, we neglect the (nearly) horizontal threads only responsible for the horizontal
101 equilibrium, which is here considered satisfied by definition.

102 The lifting of the prey did not occur immediately after the insertion of the first thread. In fact, only
103 after a given number (N_l) of attached threads the prey started to be lifted. Then the count of the
104 lifting's steps (j) started: only these N_l were considered in the vertical equilibrium of the suspended
105 body prey. We named the weight of the prey W , the thread number with the index i and the lifting's
106 step with the index j .

107 As suggested in Pugno(35) we considered two lifting strategies: all the inserted threads had the
108 same unstretched length l_{i0} (first strategy, $l_{i0}=l_0$) or after the insertion of the l_{ij} all threads changed
109 tension in order to reach the same level of strain ε_j (second strategy). Since spider silk presents an
110 initial linear elastic regime and a subsequent nonlinear elastic regime (Figure S1), we considered the

111 situation of small deformations (linear regime) and large deformations (nonlinear regime). For the
 112 former we used the following constitutive law

$$113 \quad \sigma = E\varepsilon$$

114 where E is the Young's modulus of the silk and ε its deformation. We used the following relation
 115 between ε and the initially inserted (l_{ij}) and undeformed (l_{i0}) lengths of the threads

$$116 \quad \varepsilon_{ij} = \frac{l_{ij}}{l_{i0}} - 1$$

117 The nonlinear geometrical and constitutive regime were described by the following nonlinear
 118 constitutive law(35)

$$119 \quad \sigma_{ij} = \frac{\sigma_u}{\varepsilon_u^\alpha} \ln^\alpha \left(\frac{l_{ij}}{l_{i0}} \right)$$

120 where σ_u is the ultimate strength of the silk, ε_u is the ultimate strain and α describes the power of
 121 the constitutive law: $\alpha = 1$ linear elasticity (in the limit of small strains), $\alpha > 1$ stiffening behaviour
 122 (commonly observed in natural material such as silk), $0 \leq \alpha < 1$ softening (usually observed in
 123 engineering materials).

124 The purpose of the lifting hunt mechanism is to avoid the prey escaping thanks to the lifting. For
 125 this reason, what matters the most is the vertical component of the motion of the prey.

126

127 Linear regime I strategy

128 Following Figure 2 we wrote the vertical force equilibrium between the weight of the prey and the
 129 overall vertical component of the tension generated by the threads for each lifting's step (see
 130 supplementary information). Then, following ref(35), we worked out the height of the prey at step
 131 n as a function of the measured thread angles (θ_{in} , see figure 2a)

$$132 \quad H_n = y_0 - y_n = y_0 - \frac{l_0}{E(N_I + n)} \left(\frac{W}{A} + E \sum_{i=1}^{N_I} \cos \theta_{in} + E \sum_{i=1}^n \cos \theta_{in} \right) \quad (1)$$

133

134 Linear regime II strategy

135 In this case, the length l_0 was not known but the overall strain of all the threads at each step j was
 136 known (ε_j). Again, we analysed step by step (see supplementary information) and thus obtained the
 137 height of the prey at step n as

$$138 \quad H_n = y_0 - \frac{1}{E(1 + \varepsilon_n)} \left(\frac{W}{A} + E \left(\sum_{i=1}^{N_I} \cos \theta_{in} + \sum_{i=1}^n \cos \theta_{in} \right) \right) \left(\sum_{i=1}^{N_I} \frac{1}{l_{in}} + \sum_{i=1}^n \frac{1}{l_{in}} \right)^{-1} \quad (2)$$

139

140 Nonlinear regime II strategy

141 For the sake of simplicity, we did not consider the I strategy for the nonlinear regimes.

142 Following the previous logic and the process step by step (see supplementary information) we
143 computed the height at step n

$$144 \quad H_n = y_0 - \frac{W \varepsilon_u^\alpha}{A \sigma_u} \frac{1}{\ln^\alpha(1 + \varepsilon_n)} \left(\sum_{i=1}^{N_I} \frac{1}{l_{in}} + \sum_{i=1}^n \frac{1}{l_{in}} \right)^{-1} \quad (3)$$

145 Process' efficiency

146 An efficiency was associated to the lifting process. In particular, we used a lifting velocity (final
147 height divided by the lifting time), a step efficiency $\eta = \frac{1}{n+N_I}$ (4), and a gravitational efficiency
148 (energetic efficiency) defined by Pugno(35) as following

$$149 \quad \eta' = \frac{WH}{N_I w H + w \sum_{i=1}^J y_i} \quad (5)$$

150 where w was the weight of the spider and H was the final height. The lifting velocity was calculated
151 as

$$152 \quad v = \frac{H}{t} \quad (6)$$

153 where t was the time of the whole process.

154

155 Fit the model

156 To fit the model, we used experimental values and we inserted them in the equations (1-3) by means
157 of some assumptions. The parameters inserted in the equations (1), (2) and (3) (i.e. E , σ_u , ε_u , α and
158 A) were estimated through the measure of the mechanical properties of the supporting threads
159 (lifting threads produced by major ampullate gland). The lengths and the angles of the threads were
160 measured by means of the recorded videos. For the parameter α , we extrapolated it by fitting the
161 nonlinear regions of the stress strain curves (Figure S1). Since it was impossible to measure l_{i0} , we
162 calculated it using

$$163 \quad \varepsilon = \frac{l_{ij}}{l_{i0}} - 1$$

164 where for ε we assigned two constant characteristic plausible values: one characteristic of the linear
165 elastic regime and the other of the nonlinear one, respectively 0.05 and 0.25. By fitting the model,
166 we were able to see which kind of constitutive law regime was more representative for the silk
167 during the lifting and possibly which strategy was preferred.

168

169 **Spiders, their cages and prey**

170 The spiders under study belonged to the family of Theridiidae. We used five animals: one *Steatoda*
171 *paykulliana* and four *Steatoda triangulosa*. All of these animals were kept in plastic boxes covered
172 with black paper inside at room temperature (20-23 °C and 30-39% RH) (Figure 2b,c). This was done
173 to highlight the contrast between the silk of the webs and the surrounding and thus facilitate the
174 measurements of the thread lengths and geometry. The selected prey was *Blaptica dubia*, a
175 cockroach from Central and South America. This was selected since its strength and weight (higher
176 with respect to the spider). In this context, the lifting of this animal represents a challenge for the
177 spiders under study. Each animal was weighted before the test with a high-resolution scale.

178

179 **Silk Mechanical properties**

180 From the cobwebs, we cut the trapping thread above the region covered with glue droplets. Then,
181 we glued (with a double side tape) the silk samples on a paper frame provided with a square open
182 window of 1 cm side. For tensile tests, we used a nanotensile machine (Agilent technologies T150
183 UTM) with a cell load of 500 mN. The applied strain rate was 1%/s. We computed the engineering
184 stress dividing the measured force by the cross-sectional area of each tested thread. The diameter
185 of the fibres was measured with the support of a light microscope(36), and the cross sectional area
186 of the thread (which can be composed of more fibres) was calculated using the sum of the fibres
187 cross sectional area. We present the data with the mean value and standard deviation. For *Steatoda*
188 *paykulliana* we measured ten samples of silk. For *Steatoda triangulosa* 32 (8 for each animal).

189

190 **Scanning Electron Microscopy**

191 A FE-SEM (Zeiss-40 Supra) was used to investigate the morphology of the web's junctions and
192 threads. We used a Zeiss – 40 Supra. The metallization was made by using a sputtering machine
193 Quorum Q150T and the sputtering mode was Pt/Pd 80:20 for 5 minutes.

194

195 **Measure of the thread length**

196 The lifting predation was recorded with a high-resolution Sony Camera. In order to estimate the silk
197 thread length and the height of the prey, we stopped the video when the spider attached the thread
198 to the prey and measured the length and the angles through the support of ImageJ software
199 analysis(37) (Figure 2b-c). Each parameter was measured 5 times and its mean value and standard

200 deviation computed; then we used the average for the fit. All the threads lengths and angles as well
201 as their uncertainties are reported in Supplementary data sheet. Among all the attempts in filming
202 the lifting mechanism, we selected the best five videos (see supporting videos), where these were
203 the only ones that allowed us to perform the previous mentioned quantitative analysis.
204 At each step, in this way, we had the static situation in an equilibrium point (measures of the
205 threads' lengths, their inclination, and anchorages' threads heights) that was used to fit the
206 theoretical model.

207

208 **Results**

209 **Structure of the webs**

210 The structure of the 3d cob web was complex as depicted in Figure 3a. However, some of the web's
211 components could easily be identified. With the supporting threads (Figure 3b), the spider produced
212 the main structure of the web (upper part) and it protected the den by creating a shell of these
213 threads in the frontal part of the web(19,38,39). In order to join two or more of these threads,
214 piriform and aggregate silks were used (Figure 3f) to create strong junctions(22,40). Moreover, the
215 spiders of the family Theridiidae used aggregate silk to cover capture threads with glue(41). The
216 threads were fixed to the surfaces by means of attachment discs produced by the piriform silk
217 (Figure 3d-e)(42,43). In all cases the spiders under analysis built the webs with the capture threads
218 near the bottom of the enclosure.

219

220 **Mechanical properties of the silk**

221 Figure S2 and Table 1 show the mechanical properties of the major ampullate silk (extracted from
222 supporting threads) of the spiders that were studied. The typologies of fibres are two: one for the
223 species *S. paykulliana* and one for *S. triangulosa*. We chose this type of silk because is supposed to
224 be used during the lifting(35). The silks that were analysed presented remarkable mechanical
225 properties, comparable with the ones reported in literature(44). The species of analysed spiders
226 were *Steatoda triangulosa* and *Steatoda paykulliana*. Respectively, the measured strengths were
227 205 ± 106 MPa and 409 ± 356 MPa. The strain at break was respectively 0.42 ± 0.13 and 0.26 ± 0.15 .
228 The Young's modulus was respectively 1.7 ± 1.5 GPa and 3.9 ± 3.3 GPa. The toughness modulus was
229 respectively 50 ± 39 MJ/m³ and 49 ± 41 MJ/m³. The α parameter was respectively 1.5 ± 0.5 and 1.2
230 ± 0.2 . By considering the aim of our analysis, we were interested in the ultimate stress (σ_u , i.e.
231 strength) and ultimate strain (ϵ_u) that were inserted in the equations (1-3). Thus, we used the

232 obtained mean values of these parameters for the application of the theoretical model to our
233 experimental setup. In particular, for *Steatoda triangulosa* $\varepsilon_u = 0.42$ and $\sigma_u = 205$ MPa were
234 used, whereas for *Steatoda paykulliana* $\varepsilon_u = 0.26$ and $\sigma_u = 409$ MPa were used. Moreover, the
235 cross-sectional area A was computed by summing the cross-sectional area of the fibres that
236 composed the thread (usually 2-3), which were computed using the mean value of the fibres
237 diameters (Table 1). Furthermore, in the equations the parameter $\varepsilon_n = \varepsilon = const$ is present, which
238 defines the strain of the inserted thread. Up to the model that we considered, i.e. large or small
239 deformations, the values associated to this parameter were different. In particular, for *Steatoda*
240 *paykulliana* we used $\varepsilon = 0.15$ and $\varepsilon = 0.05$ respectively; and for *Steatoda triangulosa* we used $\varepsilon =$
241 0.25 and $\varepsilon = 0.05$ respectively. These parameters were chosen on the base of the related stress
242 strain curves as representative of large or small deformations. In this regard, for large deformation
243 we considered the middle part of the second stiffening phase as the level of strain of the inserted
244 fibre. For small deformation, on the other hand, we chose the mean value of the yielding point.

245

246 **The lifting**

247 During the predation, the spiders displayed different behaviours, which can be due to the fact that
248 the prey were alive and this affected the observation.

249 In all the five selected videos (see supporting videos) when the spiders reached the prey, they
250 started to wrap it with aciniform silk(45). Moreover, when the prey reached the main frame of the
251 tangle web, the lifting was strongly affected by the presence of numerous obstacles, i.e. frame
252 threads. In this context we observed that the spiders somehow removed these obstacles. For the
253 fourth sample the prey climbed for few centimetres the wall of the cage. The lifting occurred when
254 it fell down and the spider started to wrap it.

255 For calculating the distance between the anchorage and the prey (namely y_j) we measured the
256 length of the inserted thread and the (cosine of the) angle between the thread and the vertical axes
257 (Figure 2). All the lengths and angles values as well as their uncertainties are reported in
258 Supplementary data sheets. The height H of the prey is the distance between the cockroach and the
259 ground level. These measurements were performed for each set of threads for all taken videos.

260 In all the cases the lifting did not occur immediately after the insertion of the first thread. On the
261 other hand, they started after N_i threads, which are listed in Table S1. During the predation
262 behaviours, as depicted in Figure S3, the inserted fibres were all different in term of lengths for all
263 the spiders and no apparently regularity was observed (for the values and the uncertainties see

264 supplementary data sheet). In this regard, Table S1 shows the number of threads used to lift the
265 prey ($n+N_i$, which was considered in the theoretical model), their mean length and the final height
266 reached by the prey. For the cases under study, i.e. *Steatoda triangulosa* I, *Steatoda triangulosa* II,
267 *Steatoda triangulosa* III, *Steatoda triangulosa* IV, and *Steatoda paykulliana* we observed
268 respectively $n+N_i$ equal to 29 ($N_i=5$), 73 ($N_i=13$), 47 ($N_i=11$), 34 ($N_i=3$), and 17 ($N_i=13$). Respectively,
269 the masses of the spider (and related prey) were 0.14 ± 0.01 g (0.31 ± 0.01 g), 0.04 ± 0.01 g ($0.34 \pm$
270 0.01 g), 0.02 ± 0.01 g (0.34 ± 0.01 g), 0.01 ± 0.01 g (0.50 ± 0.01 g), and 0.22 ± 0.01 g (0.36 ± 0.01 g).
271 Furthermore, it is interesting to notice the final height of the lifted prey. Comparing it with respect
272 to the height profile of the tangle web main structure (Figure S4) it is possible to notice that the final
273 height was quite close to the height profile of the main structure, but not higher. In particular, the
274 final heights that we detected were respectively 5.70 ± 2.39 cm, 4.30 ± 2.07 cm, 3.00 ± 1.73 cm, 5.40
275 ± 2.30 cm, 0.80 ± 0.35 cm (Table S1). The reason of this could be the dense net of silk fibres in the
276 main frame of cob webs, which obstructed the lifting.

277 During lifting, spiders used different anchorages where they secured the threads. Equations (1), (2),
278 and (3) require that the value of the anchorages' height is constant. In Figure S5 the measured height
279 of the anchorages and the height of the prey are depicted and it is possible to see that the height of
280 the anchorages did not change considerably during the process.

281 The predation was considered finished when the spiders stopped its lifting activity.

282

283 **The mechanics of lifting: theory compared to experiments**

284 To compare the experimental and theoretical results we neglected, for the sake of simplicity, the
285 viscoelastic relaxation of the silk for. This could be considered a reasonable ansatz since the low
286 timing of the lifting, i.e. ~10 minutes.

287 We have analysed the lifting mechanics firstly by considering the real efficiency described in
288 equation (4) with the gravitational efficiency described in equation (5). Moreover, the mean lifting
289 velocity has been associated to every lifting experiment (equation (6)). Table 2 shows the values of
290 these parameters and also the mass of the spiders and the cockroaches that were lifted.

291 In particular, the spider that shown the highest absolute efficiency η was the *Steatoda paykulliana*
292 (0.06). On the other hand, *Steatoda triangulosa* presented comparable values (namely 0.04, 0.02,
293 0.03, 0.03). In term of gravitational efficiency, the obtained values were more inhomogeneous, and
294 respectively we obtained 0.11, 0.06, 0.08, 0.32, and 0.08. The fourth spider had the highest
295 gravitational efficiency because it was the spider that lifted, relatively speaking, the heaviest prey.

296 In particular, the weight of the quarry was 50 times the spiders. The slowest lifting process (lifting
297 velocity, i.e. equation (6)) was the one of *Steatoda paykulliana* (the lowest final height was observed
298 for this spider). Respectively, the obtained velocities were 0.0046 cm/s, 0.0021 cm/s, 0.0039 cm/s,
299 0.0117 cm/s, and 0.0007 cm/s.

300 To compare the theoretical model with the experimental data we used equations (1), (2) and (3).
301 We firstly measured the mechanical properties of the spider silks involved. Then, at the end of each
302 step (equilibrium state), we measured the threads length, their inclination and the height of the
303 prey. The obtained data were inserted in the previous mentioned equations that were compared to
304 the actual lifting experiments. The comparison among the theoretical models (i.e. linear regimes I
305 and II, and nonlinear regime II) and the experimental data is depicted in Figure 4 and Figure S6. The
306 difference between the two strategies in the linear regimes was small and no major differences
307 occurred. A discrepancy between the predicted linear models and the experimental values was
308 noticed at high step's number. This discrepancy (as well as the decrease in height) is due to the fact
309 that in the theoretical model the experimental thread lengths and angles values were inserted.
310 These are affected by uncertainties (see supplementary data sheet) and thus our comparison is not
311 a best fit.

312 As highlighted in Pugno(35), the nonlinear regime improves the efficiency of the lifting especially in
313 the first lifting's steps. With the exception of the last case (*Steatoda paykulliana*), we noticed that
314 the assumption of the linear regime of the silk fitted better the experimental results. This means
315 that *Steatoda triangulosa* did not stretch the silk's threads till large deformations and only the
316 assumption of the linear regime was self-consistent with the experimental observations. It is
317 possible that this occurs because silk threads deformed and kept in the linear elastic regimes are
318 better in bearing loads cycles, with a small hysteresis(46–49). This is beneficial for hunting
319 mechanisms that involved extremely large prey that usually do not die immediately and, thus, fight
320 for their lives.

321

322 **Discussion and Conclusion**

323 Some spiders lift objects, to build den(29,31,32,34), and animals to feed(20,21,25). Theridiid spiders
324 (Figure 1a) are able to catch prey much larger and stronger than them (e.g. small lizards, small
325 mammals or big insects) by lifting them and, thus, making them immobilized since unable to hold
326 on to the underlying surface(24,25) (Figure 1b). Whilst this mechanism is not used for small
327 (medium) sized prey, which are lifted by using only the gumfoot threads and the elastic energy

328 stored in it and in the related part of the cobweb(20,21,42), it represents an interesting example of
329 how spiders are able to outperform their muscles limits. Nevertheless, in the case of extremely large
330 prey, the elastic energy stored in the cobweb and the gumfoot threads may be not sufficient for the
331 lifting and thus a multiple step lifting mechanisms is adopted.

332 In this work, we observed and quantified in the laboratory the lifting mechanism in its extreme
333 condition, which was observed before only in situ and for inanimate objects(27). The process
334 requires the use of silk with good mechanical performances(6,7) (Table 1) and the support of a
335 robust 3D cobweb(20) (Figure 3). In fact, by attaching pre-tensioned silk threads (probably
336 produced by major ampullate gland), the spider is able to apply a sum of tension that wins the prey's
337 weight (Figure 1c-f). The lifting is not abrupt and it requires many steps, forcing the spider to
338 continuously going upward and downward the web. Also, the aciniform silk(45) as well as the venom
339 are used to further immobilize the quarry during the process. This ended when the prey was close
340 to the main frame of the tangle web, where the den of the spider lies but the dense silk fibres'
341 network obstructs the movements of the quarry. This could be a reason why in the case of *Steatoda*
342 *paykulliana* less steps and lower final heights were observed, since the main structure of its cobweb
343 was particularly low (Figure S4). Moreover, since also part of the cob web (and not only the threads
344 that are directly involved in the lifting) is indirectly involved in the hunt by releasing the related
345 stored elastic energy(20), we do not exclude that a denser and larger mesh would improve the lifting
346 mechanism. A comparison between the experimental results and the theoretical model of spider
347 lifting mechanics(35) was performed under two main different hypotheses, i.e. small linear or large
348 nonlinear deformations, suggesting that in our experiments the threads are working in linear
349 regime.

350 In the lifting of objects (such as shells or leaves or living preys), spiders may achieve higher lifting
351 efficiency because of the nonlinear constitutive law of silk (i.e. large deformations)(35). However, in
352 our work with living prey, we observed that the linear strategy seems to be more compatible with
353 the observations especially for *Steatoda triangulosa* (Figure 4). Thus, the silk used during the lifting
354 by these spiders is probably kept in the linear elastic regimes (i.e. small deformations) (Figure S1).
355 In this way, the threads are able to recover and restore better the original mechanical properties
356 during loads cycles (due to the prey movement and lifting)(46,50). Interestingly, this seems in
357 countertrend with respect to the passive hunting mechanisms of the orb webs(10), in which
358 nonlinear behaviours are beneficial for both absorbing the kinetic energy of the prey and for
359 reducing the damage in the web after the impacts(9).

360 Thus, it seems that Theridiid spiders are able to use the web and their silk as an external tool to
361 hunt, which can be tuned by the arachnid. In this context, the use of silk as an external tool to store
362 elastic energy is not limited to Theridiid spiders. *Hyptiotes cavatus*, for example, uses its web as a
363 power amplification to capture flying prey, which offers many advantages over the muscles
364 limitations(11).

365 Although the experimental results are affected by large uncertainties as well as the theoretical
366 model compare simple strategies, we provide the first quantitative observation of this spider lifting
367 mechanisms for hunting living large preys. In conclusion, the spider lifting is emerging as another
368 key mechanism of the spiders that use naturally pre-stretched silk as an external tool (here like a
369 pulley) to perform actions that are impossible only with their muscles. Thus, also for lifting, the silk
370 threads seem to have a central role in spider's life and evolution.

371

372 **Acknowledgements**

373 GG and NMP would like to thank Rainer Foelix for his comments and suggestions.

374 GG would like to thank Victor Kang for his comments and suggestions and Matteo Colombo
375 for the precious help in performing experimental activity as well as Luigi Lenzini for the
376 productive discussions. The authors would like to thank Lorenzo Moschini, Prof. Antonella
377 Motta and Prof. Claudio Migliaresi (Biotech – Mattarello, University of Trento) for their
378 support with SEM facility. N.M.P. is supported by the European Commission under the FET
379 Proactive (“Neurofibres”) grant No. 732344, the FET Open (Boheme) grant No. 863179 as well as by
380 the Italian Ministry of Education, University and Research (MIUR) under the “Departments of
381 Excellence” grant L. 232/2016, the ARS01- 01384-PROSCAN and the PRIN-20177TTP3S grants. GG is
382 supported by this last grant.

383

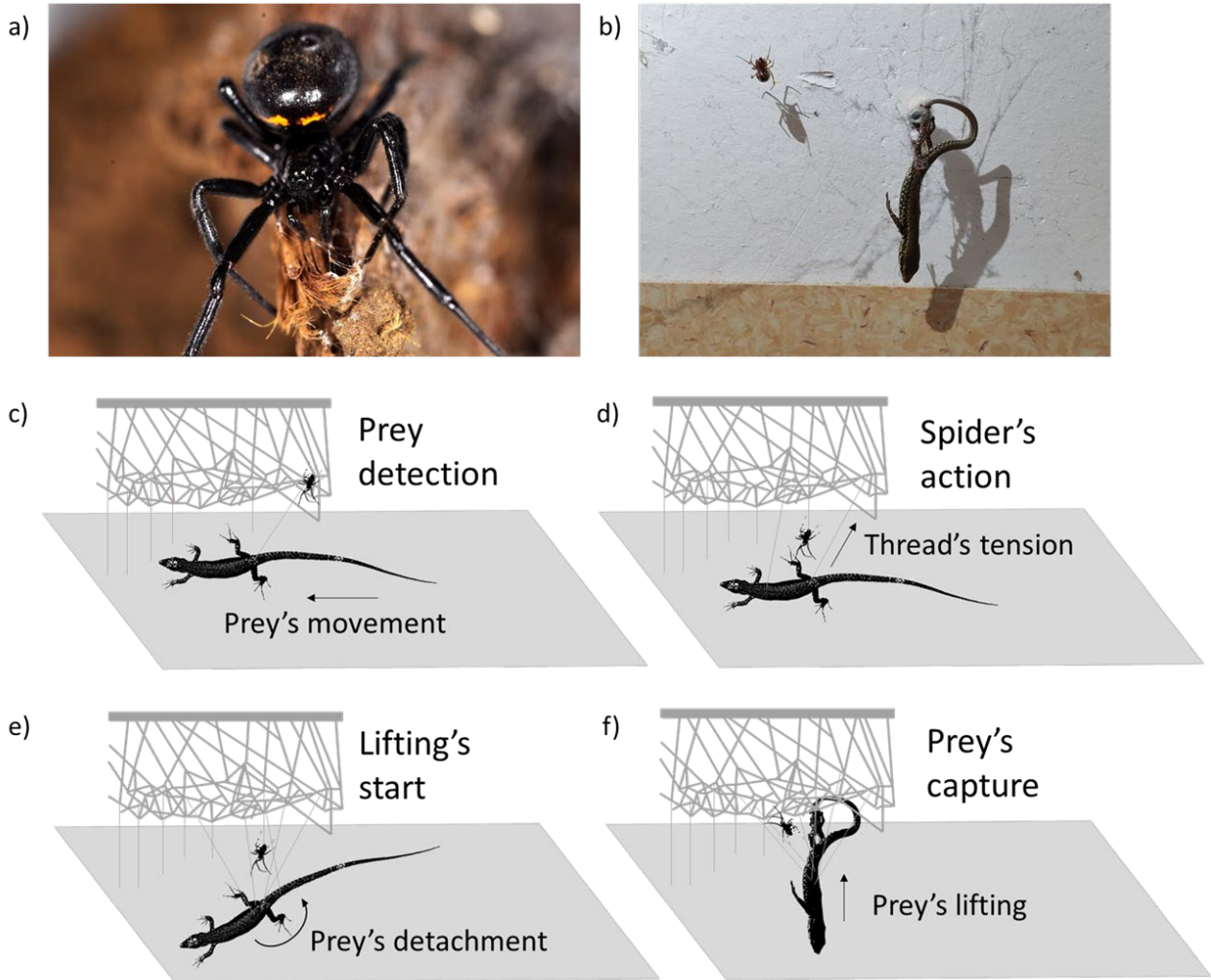
384 **Author Contributions**

385 G.G. performed the experiments, acquired the data and wrote the first draft of the paper. N.M.P.
386 suggested the idea, supervised the work, helped in the data's analysis and in the writing of the
387 manuscript. All authors viewed and approved the final manuscript and had the opportunity to
388 comment on earlier drafts.

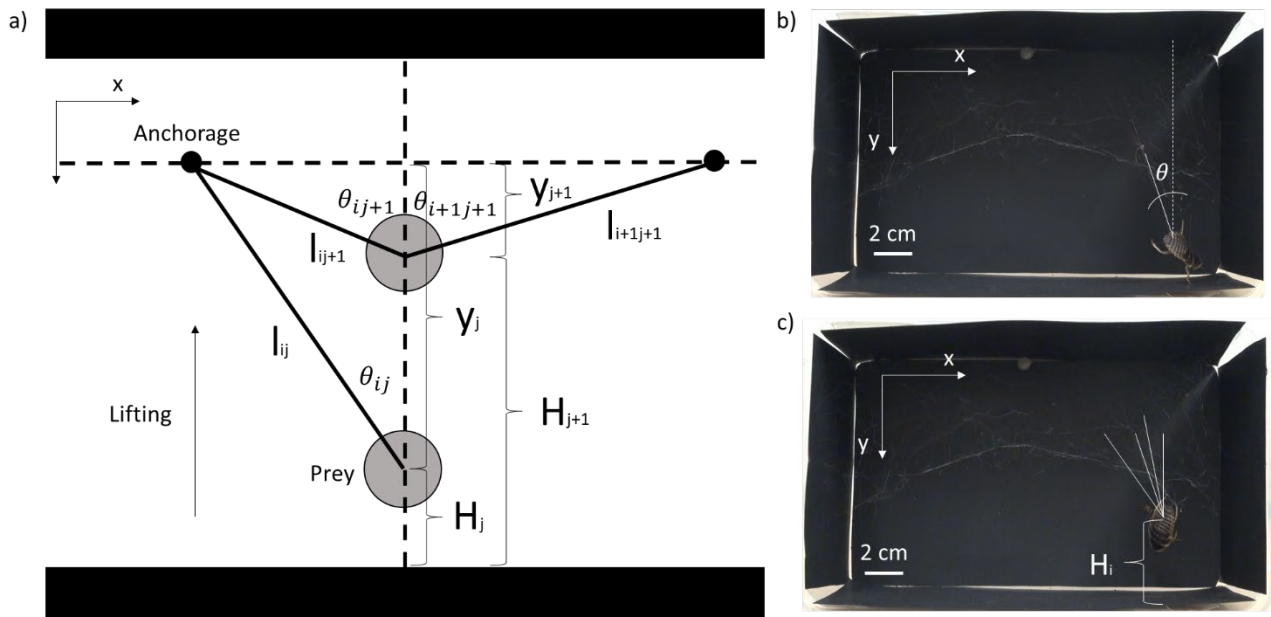
389 **Additional Information**

390 **Competing Interests:** The authors declare that they have no competing interests.

391 **Data availability:** The authors declare that the data supporting the findings of this study
392 are available within the article and its supplementary information files.

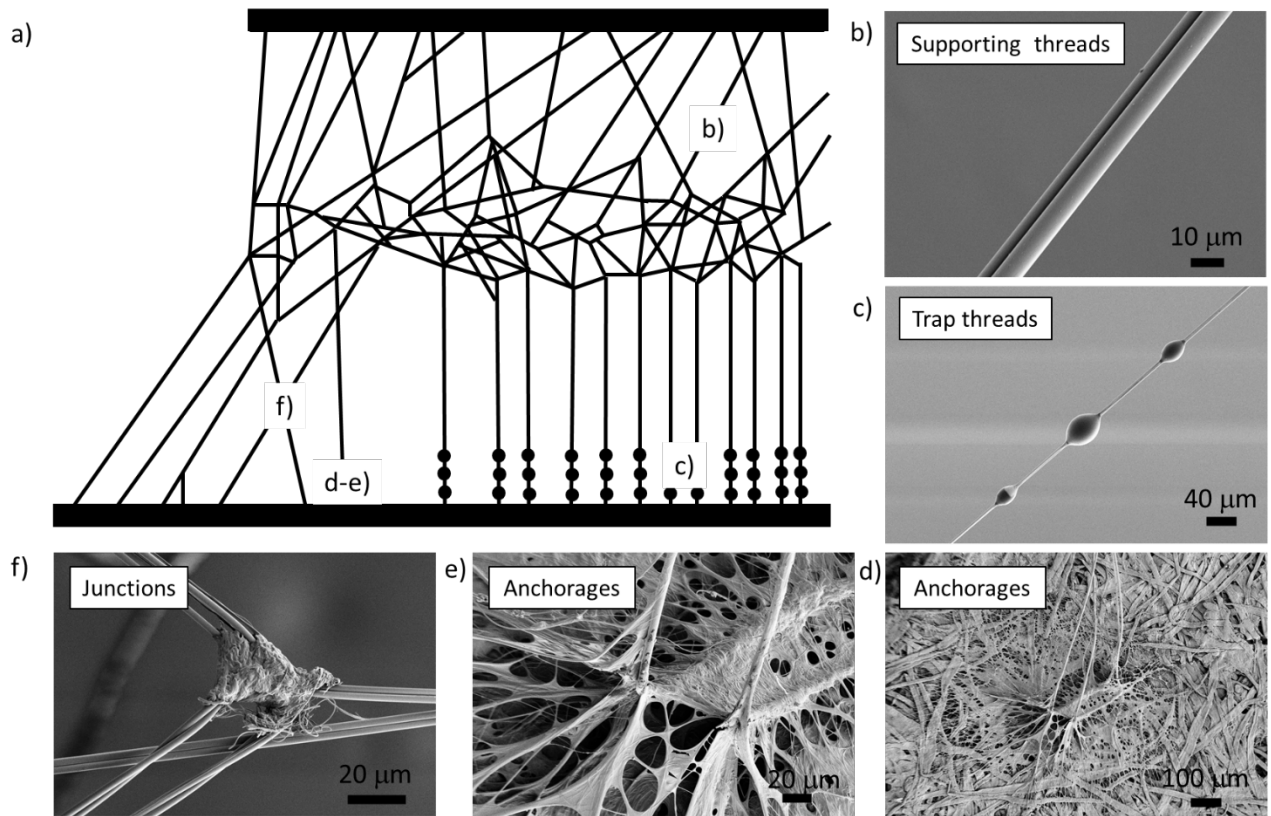


393
394 *Figure 1: a) An adult Steatoda paykuliana female of the family of Theridiidae (courtesy of Alessandro Kulczycki, Aracnofilia – The*
395 *Italian Association of Arachnology). b) A Steatoda triangulosa that captured a Lizard (Podarcis muralis) by using lifting technique*
396 *(courtesy of Emanuele Olivetti). Schematic of the technique used to lift the prey. c) the prey is detected by the capturing threads and,*
397 *once it is, d) the spider starts to attach pre-tensioned threads to it. e) When the weight of the prey is won by vertical component of*
398 *the sum of the tensions the prey detaches from the surface and f) starts to be lifted.*



399
400
401
402

Figure 2: a) Schematic of the lifting process. b) First step of the lifting process with the frame. c) After several steps the prey is lifted and the final height is H_i . This is achieved by using various threads.



403
404
405
406
407
408
409
410

Figure 3: a) Typical structure of a cob web produced by the spiders of the family Theridiidae (adapted from (51)). b) Supporting threads are produced mainly by using Macro Ampullate gland. c) Trapping threads of the web placed close to the ground in order to catch the prey. The glue is produced by aggregate gland and the main thread by major ampullate gland. d) The anchorage of the webs with the paper and e) a detail of the anchorage. f) Junctions that connect different frame threads on the web produced by piriform and aggregate gland.

Table 1: The mechanical properties of the catching thread (without glue) of the three species of spiders studied.

| Species | Nr. Samples | Fibre diameter (μm) | Strain at break (mm/mm) | Strength (MPa) | Young's modulus (GPa) | Toughness modulus (MJ/m^3) | Alpha α |
|---------|-------------|----------------------------------|-------------------------|----------------|-----------------------|--|----------------|
|---------|-------------|----------------------------------|-------------------------|----------------|-----------------------|--|----------------|

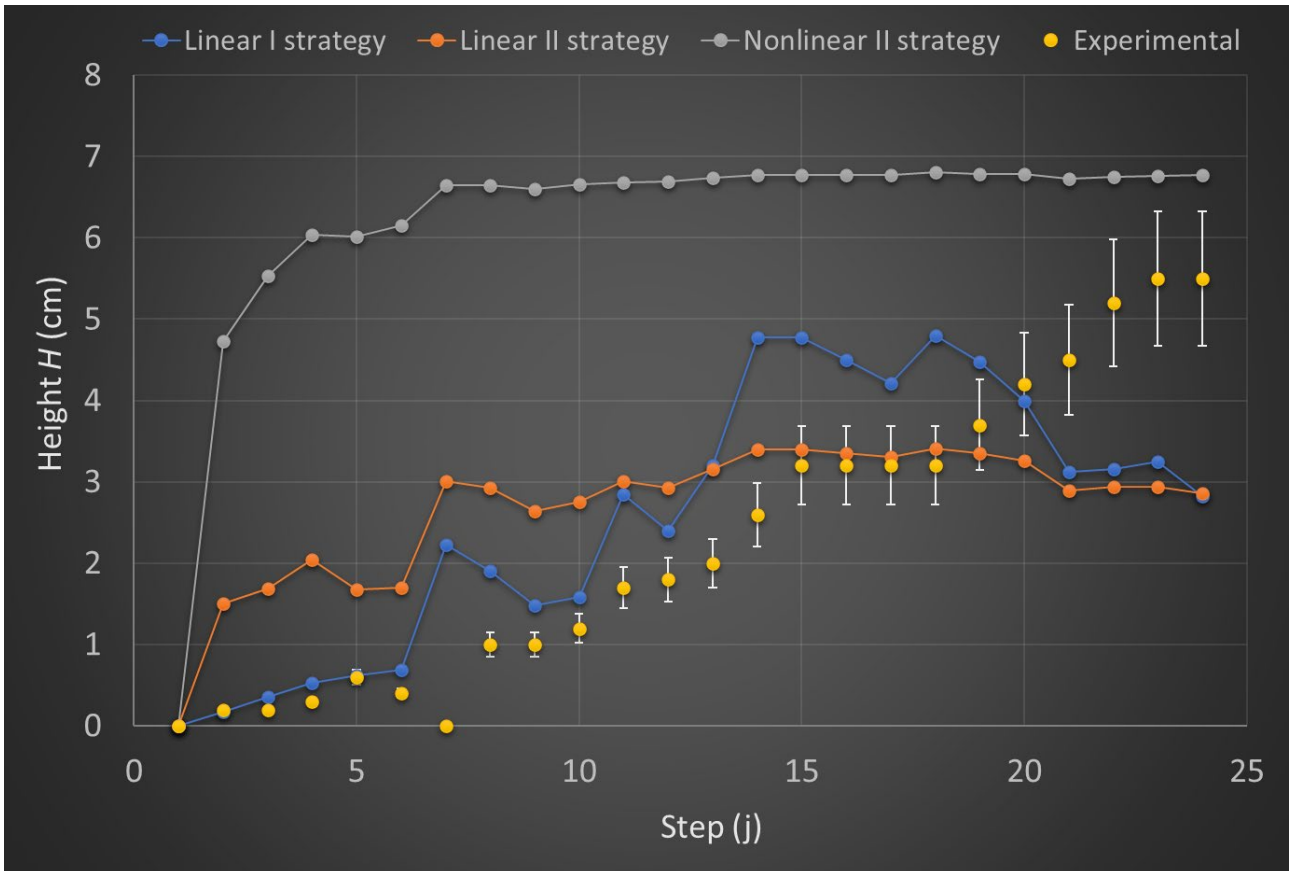
| | | | | | | | |
|-----------------------------|----|-----|-------------|-----------|-----------|---------|-----------|
| <i>Steatoda triangulosa</i> | 32 | 5±2 | 0.42 ± 0.13 | 205 ± 106 | 1.7 ± 1.5 | 50 ± 39 | 1.5 ± 0.5 |
| <i>Steatoda paykulliana</i> | 10 | 7±2 | 0.26 ± 0.15 | 409 ± 356 | 3.9 ± 3.3 | 49 ± 41 | 1.2 ± 0.2 |

411
412
413

Table 2: The efficiencies and velocities of the lifting of the different cases analysed in this study. η indicate the process' efficiency and η' indicate the gravitational efficiency and V the lifting velocity.

| Spider | Mass of the spider (g) | Mass of the <i>Blaptica dubia</i> (g) | η | η' | V (cm/s) |
|--------------------------------|------------------------|---------------------------------------|--------|---------|------------|
| <i>Steatoda triangulosa</i> 1° | 0.14 ± 0.01 | 0.31 ± 0.01 | 0.04 | 0.11 | 0.0046 |
| <i>Steatoda triangulosa</i> 2° | 0.04 ± 0.01 | 0.34 ± 0.01 | 0.02 | 0.06 | 0.0021 |
| <i>Steatoda triangulosa</i> 3° | 0.02 ± 0.01 | 0.34 ± 0.01 | 0.03 | 0.08 | 0.0039 |
| <i>Steatoda triangulosa</i> 4° | 0.01 ± 0.01 | 0.50 ± 0.01 | 0.03 | 0.32 | 0.0117 |
| <i>Steatoda paykulliana</i> | 0.22 ± 0.01 | 0.36 ± 0.01 | 0.06 | 0.08 | 0.0007 |

414



415
416
417
418

Figure 4: Representative comparison among the theoretical model and the experimental data of the lifting. Grey lines = nonlinear elastic regime (II strategy); blue lines = linear elastic regime (I strategy); orange line = linear elastic regime (II strategy); yellow line = experimental data.

419 **References**

- 420 1. Herberstein ME. Spider Behaviour: Flexibility And Versatility. 1st ed. Herberstein ME, editor.
421 Cambridge University Press; 2012. 391 p.
- 422 2. Craig LB and CL. Spider Silk Evolution and 400 Million Years of Spinning, Waiting, Snagging, and
423 Mating. Press YU, editor. London; 2012. 248 p.
- 424 3. Blackledge TA. Spider silk: a brief review and prospectus on research linking biomechanics and
425 ecology in draglines and orb webs. *J Arachnol* [Internet]. 2012;40(1):1–12. Available from:
426 <http://www.bioone.org/doi/abs/10.1636/M11-67.1>
- 427 4. Hakimi O, Knight DP, Knight MM, Grahn MF, Vadgama P. Ultrastructure of insect and spider cocoon
428 silks. *Biomacromolecules*. 2006;7(10):2901–8.
- 429 5. Scott CE, Anderson AG, Andrade MCB. A review of the mechanisms and functional roles of male silk
430 use in spider courtship and mating. *J Arachnol*. 2018;46(2):173–206.
- 431 6. Agnarsson I, Kuntner M, Blackledge TA. Bioprospecting finds the toughest biological material:
432 Extraordinary silk from a giant riverine orb spider. *PLoS One*. 2010;5(9):1–8.
- 433 7. Greco G, Pugno NM. Mechanical Properties and Weibull Scaling Laws of Unknown Spider Silks.
434 *Molecules*. 2020;25(2938).
- 435 8. Wang Z, Cang Y, Kremer F, Thomas EL, Fytas G. Determination of the Complete Elasticity of *Nephila*
436 *pilipes* Spider Silk. 2020;
- 437 9. Cranford SW, Tarakanova A, Pugno NM, Buehler MJ. Nonlinear material behaviour of spider silk
438 yields robust webs. *Nature*. 2012;482(7383):72–6.
- 439 10. Sensenig AT, Lorentz KA, Kelly SP, Blackledge TA. Spider orb webs rely on radial threads to absorb
440 prey kinetic energy. *J R Soc Interface* [Internet]. 2012;9(73):1880–91. Available from:
441 <http://rsif.royalsocietypublishing.org/cgi/doi/10.1098/rsif.2011.0851>
- 442 11. Han SI, Astley HC, Maksuta DD, Blackledge TA. External power amplification drives prey capture in a
443 spider web. *PNAS*. 2019;1–6.
- 444 12. Wainwright P, Kraklau D, Bennet A. Kinematics of tongue projection in *Chamaeleo oustaleti*. *J Exp*
445 *Biol*. 1991;159:109–33.
- 446 13. Patek S, Nowroozi B, Baio J, Caldwell R, Summers A. Linkage mechanics and power amplification of
447 the mantis shrimp's strike. *J Exp Biol*. 2007;210:3677–88.
- 448 14. Peplowski M, Marsh R. Work and power output in the hindlimb muscles of Cuban tree frogs
449 *Osteopilus septentrionalis* during jumping. *J Exp Biol*. 1997;200:2861–70.
- 450 15. Sutton G, Burrows M. Biomechanics of jumping in the flea. *J Exp Biol*. 2011;214:836–47.
- 451 16. Patek S. The most powerful movements in biology. *AM Sci*. 2015;103(330).
- 452 17. McGowan C, Baudinette R, Usherwood J, Biewener A. The mechanics of jumping versus steady
453 hopping in yellow-footed rock wallabies. *J Exp Biol*. 2005;208:2741–51.
- 454 18. Burrows M, Shaw S, Sutton G. Resilin and chitinous cuticle form a composite structure for energy
455 storage in jumping by frog hopper insects. *BMC Biol*. 2008;6(41).
- 456 19. Benjamin SP, Zschokke S. Untangling the tangle-web: Web construction behavior of the comb-
457 footed spider *Steatoda triangulosa* and comments on phylogenetic implications (Araneae:
458 Theridiidae). *J Insect Behav*. 2002;15(6):791–809.
- 459 20. Argintean S, Chen J, Kim M, Moore AMF. Resilient silk captures prey in black widow cobwebs. *Appl*
460 *Phys A*. 2006;82(2):235–41.
- 461 21. Nyffeler BM, Dean DA, Sterling WL. The southern black widow spider , *Latrodectus rnaetans* (
462 Araneae , Theridiidae), as a predator of the red imported fire ant , *Solenopsis invicta* (Hymenoptera
463 , Formicidae), in Texas cotton fields. 1988;106:52–7.
- 464 22. Vasanthavada K, Hu X, Tuton-Blasingame T, Hsia Y, Sampath S, Pacheco R, et al. Spider glue proteins
465 have distinct architectures compared with traditional spidroin family members. *J Biol Chem*.
466 2012;287(43):35985–99.
- 467 23. Choreshe O, Bayarmagnai B, Lewis R V. Spider web glue: Two proteins expressed from opposite
468 strands of the same DNA sequence. *Biomacromolecules*. 2009;10(10):2852–6.
- 469 24. Ewing HE. The life and behavior of the house spider. *Proc Iowa Acad Sci* [Internet]. 1918;46(1).
470 Available from: <https://scholarworks.uni.edu/pias/vol46/iss1/44>

- 471 25. Nyffeler M, Vetter RS. Black widow spiders, *Latrodectus* spp. (Araneae: Theridiidae), and other
472 spiders feeding on mammals . *J Arachnol.* 2018;46(3):541–8.
- 473 26. R. D, K. F, .L. K, W. D. *Natural History Notes. Herpetol Rev.* 2017;48(2):446–7.
- 474 27. Mc Cook H. *American Spiders and their spinning work.* 1889. 386 p.
- 475 28. Keown M. *Proceedings of the Royal Zoological Society of New South Wales.* 1943;89th(March):78.
476 Available from: <http://www.biodiversitylibrary.org/item/119542>
- 477 29. Bigot L. *Sur le comportement en captivité de l'araignee Olios coenobita Fage.* *C R Hebd Seance Acad*
478 *Sci.* 1969;D 268:729–30.
- 479 30. Decary R. *Notes concernant les moeurs de deux curieuses espèces d'araignées observées dans le*
480 *sud de l'île.* *Bull Acad Malgache N S IV.* 1918;20–1.
- 481 31. Decary R. *Observations sur l' Olios coenobita Fage et le Nemoscolus waterloti Berland.* *Arch Zool Exp*
482 *Gen.* 1926;65:18–21.
- 483 32. Foelix VR, Thieleczek R, Erb B. *Spinnen in Schneckenhäusern : Wie bringen sie ihre Schalen in luftige*
484 *Höhen ? ARACHNE.* 2019;
- 485 33. Decary M. *COLONIE DE MADAGASCAB ET DEPENDANCES NOUVELLE SERIE. Bulletin de l'Academie*
486 *Malgache.* 1918;Tome IV:20–1.
- 487 34. Fage L. *Sur quelques Araignées de Madagascar, nouvelles ou peu connues et sur leur curieuse*
488 *industrie.* *Arch Zool Expr Gen.* 1926;65:5–17.
- 489 35. Pugno NM. *Spider weight dragging and lifting mechanics.* *Meccanica [Internet].* 2018;53(4–5):1105–
490 14. Available from: <http://link.springer.com/10.1007/s11012-017-0787-x>
- 491 36. Blackledge TA, Cardullo RA, Hayashi CY. *Polarized light microscopy, variability in spider silk*
492 *diameters, and the mechanical characterization of spider silk.* *Invertebr Biol.* 2005;124(2):165–73.
- 493 37. Schneider CA, Rasband WS, Eliceri KW. *NIH Image to ImageJ: 25 years of image analysis.* *Nat*
494 *Methods.* 2012;9(7):671–5.
- 495 38. Benjamin SP, Zschokke S. *Webs of theridiid spiders: Construction, structure and evolution.* *Biol J Linn*
496 *Soc.* 2003;78(3):293–305.
- 497 39. Blackledge TA, Coddington JA, Gillespie RG. *Are three-dimensional spider webs defensive*
498 *adaptations?* *Ecol Lett.* 2003;6(1):13–8.
- 499 40. Greco G, Pantano MF, Mazzolai B, Pugno NM. *Imaging and mechanical characterization of different*
500 *junctions in spider orb webs.* *Sci Rep [Internet].* 2019;9(1):5776. Available from:
501 <http://www.nature.com/articles/s41598-019-42070-8>
- 502 41. Blackledge TA. *Quasistatic and continuous dynamic characterization of the mechanical properties of*
503 *silk from the cobweb of the black widow spider Latrodectus hesperus.* *J Exp Biol [Internet].*
504 2005;208(10):1937–49. Available from: <http://jeb.biologists.org/cgi/doi/10.1242/jeb.01597>
- 505 42. Sahni V, Harris J, Blackledge TA, Dhinojwala A. *Cobweb-weaving spiders produce different*
506 *attachment discs for locomotion and prey capture.* *Nat Commun [Internet].* 2012;3:1106–7.
507 Available from: <http://dx.doi.org/10.1038/ncomms2099>
- 508 43. Greco G, Wolff J, Pugno NM. *Strong and tough silk for resilient attachment discs: the mechanical*
509 *properties of piriform silk, in the spider Cupiennius salei (Keyserling, 1877).* *Front Mater.*
510 2020;7(138).
- 511 44. Blackledge TA, Summers AP, Hayashi CY. *Gumfooted lines in black widow cobwebs and the*
512 *mechanical properties of spider capture silk.* *Zoology.* 2005;108(1):41–6.
- 513 45. Hayashi CY, Blackledge TA, Lewis R V. *Molecular and mechanical characterization of aciniform silk:*
514 *Uniformity of iterated sequence modules in a novel member of the spider silk fibroin gene family.*
515 *Mol Biol Evol.* 2004;21(10):1950–9.
- 516 46. Hennecke K, Redeker J, Kuhbier JW, Strauss S, Allmeling C, Kasper C, et al. *Bundles of Spider Silk,*
517 *Braided into Sutures, Resist Basic Cyclic Tests: Potential Use for Flexor Tendon Repair.* *PLoS One.*
518 2013;8(4).
- 519 47. Kumar B, Singh KP. *Fatigueless response of spider draglines in cyclic torsion facilitated by reversible*
520 *molecular deformation.* *Appl Phys Lett.* 2014;105(21):10–5.
- 521 48. Vehoff T, Glišović A, Schollmeyer H, Zippelius A, Salditt T. *Mechanical properties of spider dragline*
522 *silk: Humidity, hysteresis, and relaxation.* *Biophys J.* 2007;93(12):4425–32.
- 523 49. Sampath S, Yarger JL. *Structural hysteresis in dragline spider silks induced by supercontraction: An X-*

524 ray fiber micro-diffraction study. RSC Adv. 2015;5(2):1462–73.
525 50. Gosline JM, Guerette PA, Ortlepp CS, Savage KN. The mechanical design of spider silks: from fibroin
526 sequence to mechanical function. J Exp Biol. 1999;202:3295–303.
527 51. Foelix R. Biology of Spiders. London: Oxford University Press; 2011.
528
529
530
531
532

533 **Supplementary information**

534 **How spiders hunt heavy prey: the tangle web as a pulley and spider's lifting**
535 **mechanics observed and quantified in the laboratory**

536 Gabriele Greco ¹, Nicola M. Pugno ^{1, 2*}

537 ¹ Laboratory of Bio-Inspired, Bionic, Nano, Meta Materials & Mechanics, Department of Civil,
538 Environmental and Mechanical Engineering, University of Trento, Via Mesiano, 77, 38123 Trento,
539 Italy

540 ² School of Engineering and Materials Science, Queen Mary University of London, Mile End Road,
541 E1 4NS London, United Kingdom

542 *Corresponding author: nicola.pugno@unitn.it

543

544

545 **The mechanical model (detailed description)**

546 Linear regime I strategy

547 Following Figure 2 we wrote the vertical force equilibrium between the weight of the prey and the
548 overall vertical component of the tension generated²¹ by the threads for each lifting's step²¹:

549 1) $\frac{W}{A} = \sum_{i=1}^{N_I} \sigma_{i1} \cos \theta_{i1} + \sigma_{11} \cos \theta_{11} = \sum_{i=1}^{N_I} \left(E \left(\frac{l_{i1}}{l_0} - 1 \right) \cos \theta_{i1} \right) + \cos \theta_{11} E \left(\frac{l_{11}}{l_0} - 1 \right) =$

550 $\sum_{i=1}^{N_I} \left(E \left(\frac{y_1}{\cos \theta_{i1} l_0} - 1 \right) \cos \theta_{i1} \right) + \cos \theta_{11} E \left(\frac{y_1}{\cos \theta_{11} l_0} - 1 \right)$

551 $\Rightarrow y_1 = \frac{l_0}{E(N_I + 1)} \left(\frac{W}{A} + E \sum_{i=1}^{N_I} \cos \theta_{i1} + E \cos \theta_{11} \right)$

552 where A is the cross-sectional area of the silk thread (considered constant during the process) and
553 y_i is the vertical distance between the prey and the anchorage of the thread. The first sum (till N_I)
554 of vertical components of the threads' tensions was related to the silk fibres inserted prior to lifting.

555 The next step was described as follow²¹:

556 2) $\frac{W}{A} = \sum_{i=1}^{N_I} \sigma_{i2} \cos \theta_{i2} + \sigma_{12} \cos \theta_{12} + \sigma_{22} \cos \theta_{22} = \sum_{i=1}^{N_I} \left(E \left(\frac{l_{i2}}{l_0} - 1 \right) \cos \theta_{i2} \right) +$

557 $\cos \theta_{12} E \left(\frac{l_{12}}{l_0} - 1 \right) + \cos \theta_{22} E \left(\frac{l_{22}}{l_0} - 1 \right) = \sum_{i=1}^{N_I} \left(E \left(\frac{y_2}{\cos \theta_{i2} l_0} - 1 \right) \cos \theta_{i2} \right) +$

558 $+ \cos \theta_{12} E \left(\frac{y_2}{\cos \theta_{12} l_0} - 1 \right) + \cos \theta_{22} E \left(\frac{y_2}{\cos \theta_{22} l_0} - 1 \right)$

559 $\Rightarrow y_2 = \frac{l_0}{E(N_I + 2)} \left(\frac{W}{A} + E \sum_{i=1}^{N_I} \cos \theta_{i2} + E(\cos \theta_{12} + \cos \theta_{22}) \right)$

560 ...

561 n) $y_n = \frac{l_0}{E(N_I + n)} \left(\frac{W}{A} + E \sum_{i=1}^{N_I} \cos \theta_{in} + E \sum_{i=1}^n \cos \theta_{in} \right)$

562 If the height of the anchorages is constant during the process, we calculated the height of the prey
 563 at the lifting's step n by using²¹:

$$564 \quad H_n = y_0 - y_n = y_0 - \frac{l_0}{E(N_I + n)} \left(\frac{W}{A} + E \sum_{i=1}^{N_I} \cos \theta_{i1} + E \sum_{i=1}^n \cos \theta_{in} \right) \quad (1)$$

565 Linear regime II strategy

566 We proceed by following the previous logic scheme. However, this time the length l_0 was not known
 567 but the overall strain of all the threads at each step j was known (ε_j). Again, we analysed step by
 568 step and thus we obtained²¹:

$$569 \quad 1) \frac{W}{A} = \sum_{i=1}^{N_I} \sigma_{i1} \cos \theta_{i1} + \sigma_{11} \cos \theta_{11} = \sum_{i=1}^{N_I} E \cos \theta_{i1} \left(\frac{l_{i1}}{l_{i0}} - 1 \right) + E \cos \theta_{11} \left(\frac{l_{11}}{l_{10}} - 1 \right) =$$

$$570 \quad \sum_{i=1}^{N_I} \frac{E y_1}{l_{i1}} (1 + \varepsilon_1) - E \sum_{i=1}^{N_I} \cos \theta_{i1} + \frac{E y_1}{l_{11}} (1 + \varepsilon_1) - E \cos \theta_{11}$$

$$571 \quad \Rightarrow y_1 = \frac{1}{E(1 + \varepsilon_1)} \left(\frac{W}{A} + E \left(\sum_{i=1}^{N_I} \cos \theta_{i1} + \cos \theta_{11} \right) \right) \left(\sum_{i=1}^{N_I} \frac{1}{l_{i1}} + \frac{1}{l_{11}} \right)^{-1}$$

572 where first sum (till N_I) of vertical components of the threads' tensions is related to the silk fibres
 573 inserted prior to lifting. The next step is described as follow²¹:

$$574 \quad 2) \frac{W}{A} = \sum_{i=1}^{N_I} \sigma_{i2} \cos \theta_{i2} + \sigma_{12} \cos \theta_{12} + \sigma_{22} \cos \theta_{22} = \sum_{i=1}^{N_I} E \cos \theta_{i2} \left(\frac{l_{i2}}{l_{i0}} - 1 \right) +$$

$$575 \quad E \cos \theta_{12} \left(\frac{l_{12}}{l_{10}} - 1 \right) + E \cos \theta_{22} \left(\frac{l_{22}}{l_{20}} - 1 \right) = \sum_{i=1}^{N_I} \frac{E y_2}{l_{i2}} (1 + \varepsilon_2) - E \sum_{i=1}^{N_I} \cos \theta_{i2} + \frac{E y_2}{l_{12}} (1 +$$

$$576 \quad \varepsilon_2) - E \cos \theta_{12} + \frac{E y_2}{l_{22}} (1 + \varepsilon_2) - E \cos \theta_{22}$$

$$577 \quad \Rightarrow y_2 = \frac{1}{E(1 + \varepsilon_2)} \left(\frac{W}{A} + E \left(\sum_{i=1}^{N_I} \cos \theta_{i2} + \cos \theta_{12} + \cos \theta_{22} \right) \right) \left(\sum_{i=1}^{N_I} \frac{1}{l_{i2}} + \frac{1}{l_{12}} + \frac{1}{l_{22}} \right)^{-1}$$

578 ...

$$579 \quad n) y_n = \frac{1}{E(1 + \varepsilon_n)} \left(\frac{W}{A} + E \left(\sum_{i=1}^{N_I} \cos \theta_{in} + \sum_{i=1}^n \cos \theta_{in} \right) \right) \left(\sum_{i=1}^{N_I} \frac{1}{l_{in}} + \sum_{i=1}^n \frac{1}{l_{in}} \right)^{-1}$$

580 If the height of the anchorages is constant during the process, we can compute the height of the
 581 prey at the lifting's step n by using²¹:

$$582 \quad H_n = y_0 - \frac{1}{E(1 + \varepsilon_n)} \left(\frac{W}{A} + E \left(\sum_{i=1}^{N_I} \cos \theta_{in} + \sum_{i=1}^n \cos \theta_{in} \right) \right) \left(\sum_{i=1}^{N_I} \frac{1}{l_{in}} + \sum_{i=1}^n \frac{1}{l_{in}} \right)^{-1} \quad (2)$$

583

584 Nonlinear regime II strategy

585 For the sake of simplicity, we do not consider the I strategy for the nonlinear regimes.

586 Following the previous logic and the process step by step we obtained²¹:

587 1) $\frac{W}{A} = \sum_{i=1}^{N_I} \sigma_{i1} \cos \theta_{i1} + \sigma_{11} \cos \theta_{11} = \sum_{i=1}^{N_I} \cos \theta_{i1} \frac{\sigma_u}{\varepsilon_u^\alpha} \ln^\alpha \left(\frac{l_{i1}}{l_{i0}} \right) + \cos \theta_{11} \frac{\sigma_u}{\varepsilon_u^\alpha} \ln^\alpha \left(\frac{l_{11}}{l_{10}} \right) =$

588 $\sum_{i=1}^{N_I} \frac{y_1 \sigma_u}{l_{i1} \varepsilon_u^\alpha} \ln^\alpha(1 + \varepsilon_1) + \frac{y_1 \sigma_u}{l_{11} \varepsilon_u^\alpha} \ln^\alpha(1 + \varepsilon_1)$

589 $\Rightarrow y_1 = \frac{W \varepsilon_u^\alpha}{A \sigma_u \ln^\alpha(1 + \varepsilon_1)} \left(\sum_{i=1}^{N_I} \frac{1}{l_{i1}} + \frac{1}{l_{11}} \right)^{-1}$

590 where first sum (till N_I) of vertical components of the threads' tensions was related to the silk fibres
591 inserted prior to lifting. The next step was described as follow²¹:

592 2) $\frac{W}{A} = \sum_{i=1}^{N_I} \sigma_{i2} \cos \theta_{i2} + \sigma_{12} \cos \theta_{12} + \sigma_{22} \cos \theta_{22} = \sum_{i=1}^{N_I} \cos \theta_{i2} \frac{\sigma_u}{\varepsilon_u^\alpha} \ln^\alpha \left(\frac{l_{i2}}{l_{i0}} \right) +$

593 $\cos \theta_{12} \frac{\sigma_u}{\varepsilon_u^\alpha} \ln^\alpha \left(\frac{l_{12}}{l_{10}} \right) + \cos \theta_{22} \frac{\sigma_u}{\varepsilon_u^\alpha} \ln^\alpha \left(\frac{l_{22}}{l_{20}} \right) = \sum_{i=1}^{N_I} \frac{y_2 \sigma_u}{l_{i2} \varepsilon_u^\alpha} \ln^\alpha(1 + \varepsilon_2) + \frac{y_2 \sigma_u}{l_{12} \varepsilon_u^\alpha} \ln^\alpha(1 + \varepsilon_2) +$

594 $\frac{y_2 \sigma_u}{l_{22} \varepsilon_u^\alpha} \ln^\alpha(1 + \varepsilon_2)$

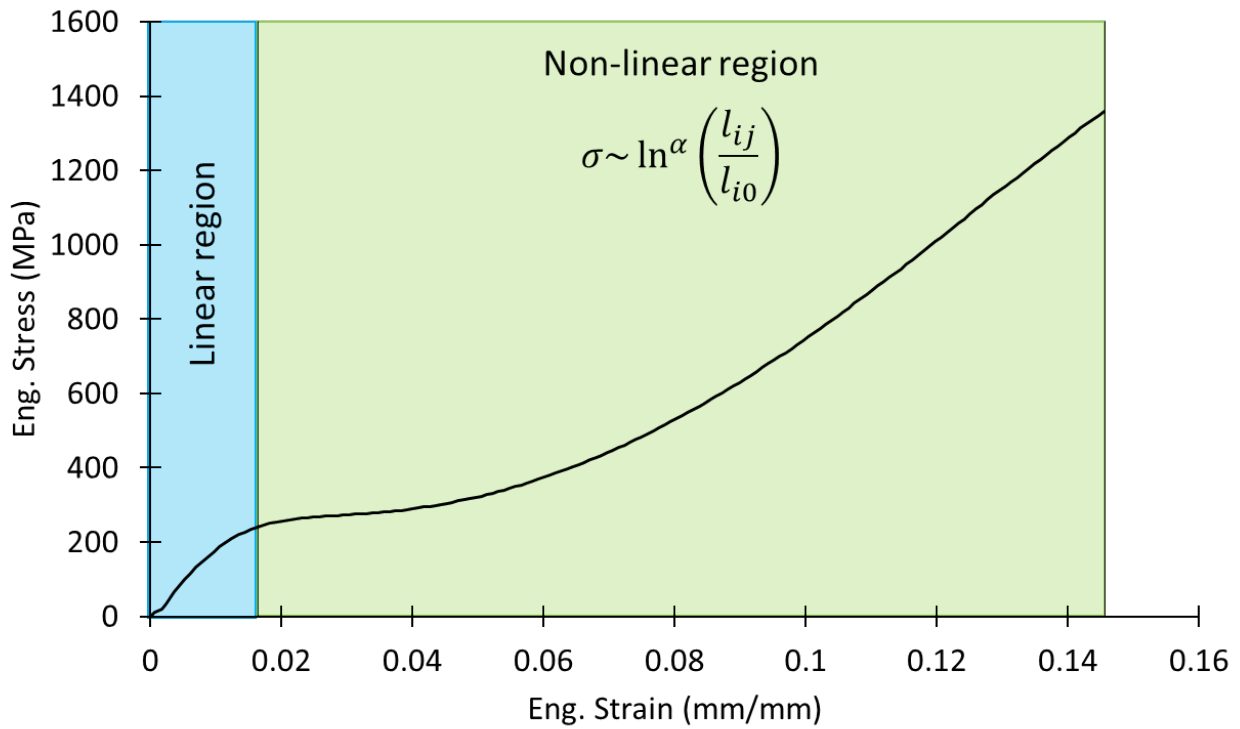
595 $\Rightarrow y_2 = \frac{W \varepsilon_u^\alpha}{A \sigma_u \ln^\alpha(1 + \varepsilon_2)} \left(\sum_{i=1}^{N_I} \frac{1}{l_{i2}} + \frac{1}{l_{12}} + \frac{1}{l_{22}} \right)^{-1}$

596 ...

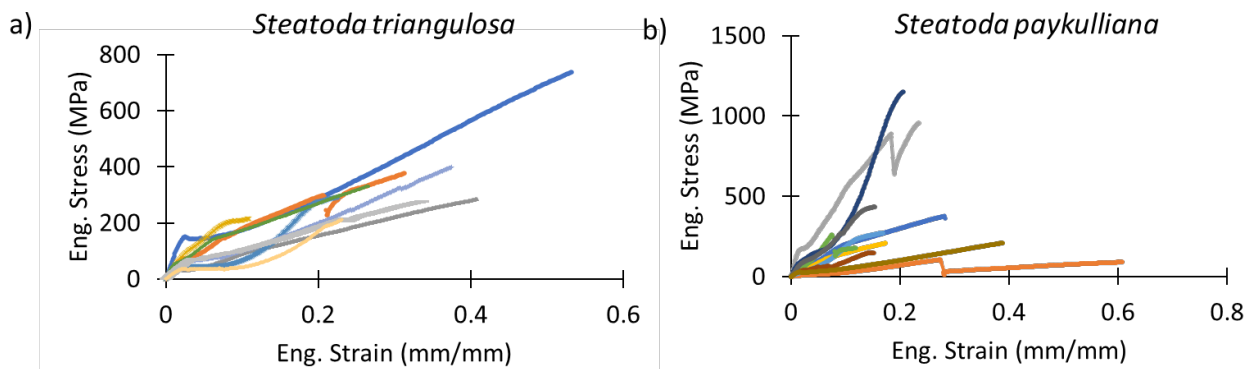
597 n) $y_n = \frac{W \varepsilon_u^\alpha}{A \sigma_u \ln^\alpha(1 + \varepsilon_n)} \left(\sum_{i=1}^{N_I} \frac{1}{l_{in}} + \sum_{i=1}^n \frac{1}{l_{in}} \right)^{-1}$

598 If the height of the anchorages is constant during the process, we can compute the height of the
599 prey at the lifting's step n by using²¹:

600 $H_n = y_0 - \frac{W \varepsilon_u^\alpha}{A \sigma_u \ln^\alpha(1 + \varepsilon_n)} \left(\sum_{i=1}^{N_I} \frac{1}{l_{in}} + \sum_{i=1}^n \frac{1}{l_{in}} \right)^{-1} \quad (3)$



601
 602 Figure S1: A typical stress strain curve of a spider silk fibre. In order to compute α , we fit the nonlinear region with the indicated
 603 equation. The first region, on the other hand, is the linear one.

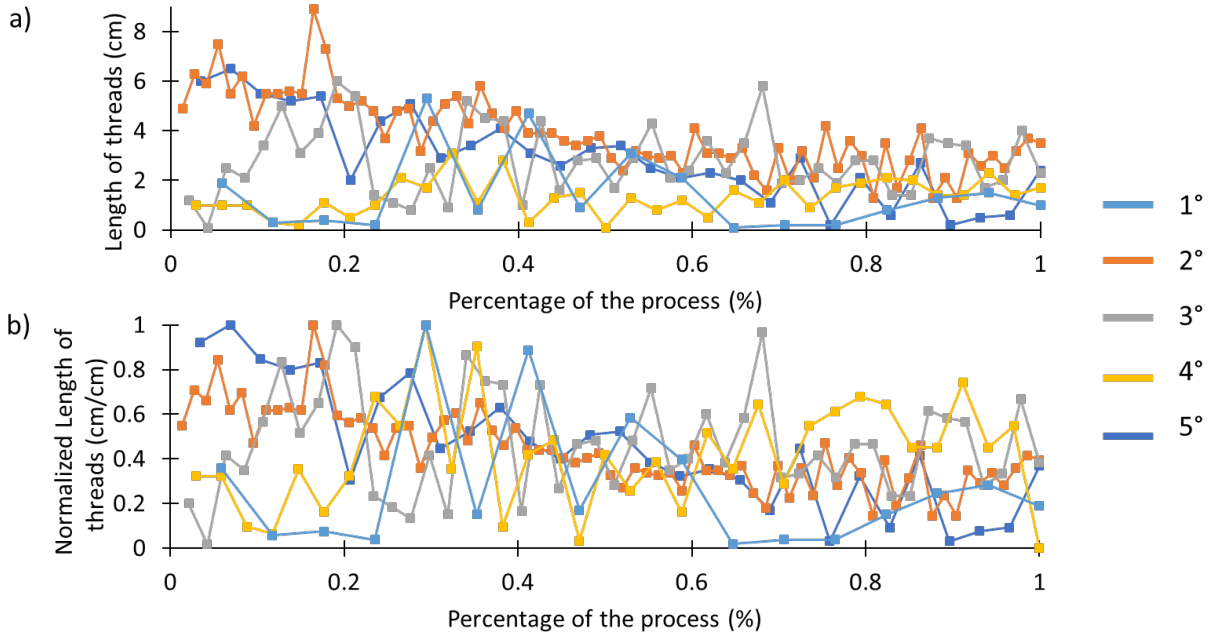


604
 605 Figure S2: The mechanical properties of the catching thread (without glue) of the two species of spiders that were studied. a) Stress-
 606 strain curves of the species *Steatoda triangulosa*, b) stress-strain curves of the species *Steatoda paykulliana*.
 607

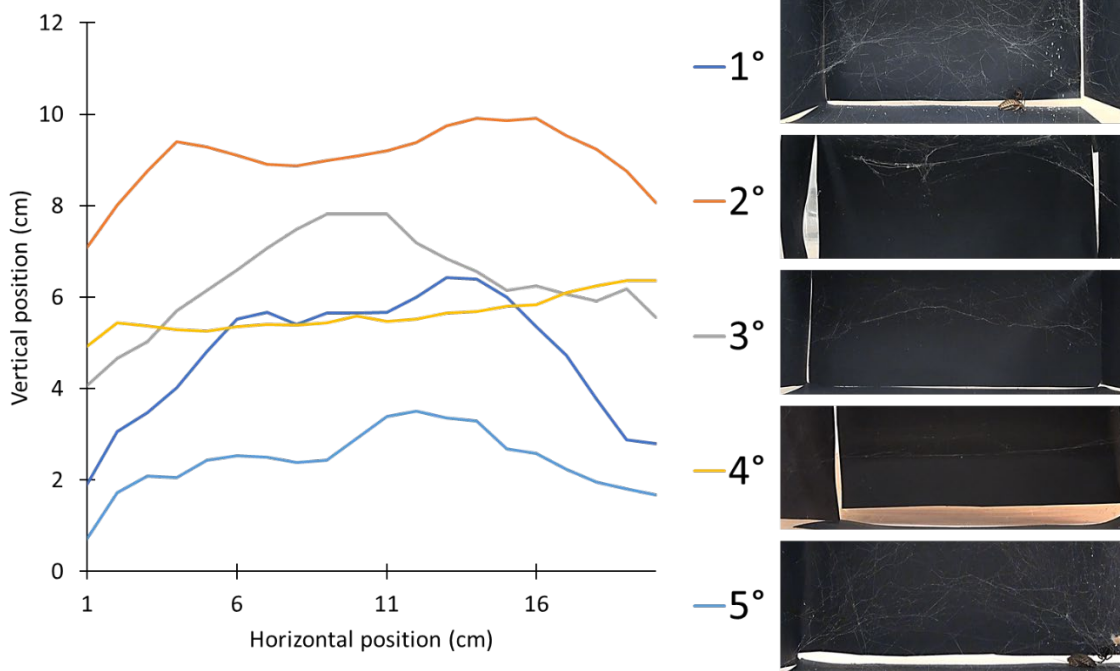
608 Table S1: The number of threads used (whole process) to lift the prey, their mean length and the final height at which the prey is lifted
 609 at the end of the process. N_i is the number of threads inserted prior the lifting and n is the number of threads inserted during the
 610 lifting.

| Spider | Number of used threads | | Final Height (cm) |
|--------------------------------|------------------------|-----|-------------------|
| | N_i | n | |
| <i>Steatoda triangulosa</i> 1° | 5 | 24 | 5.70 ± 2.39 |
| <i>Steatoda triangulosa</i> 2° | 13 | 60 | 4.30 ± 2.07 |
| <i>Steatoda triangulosa</i> 3° | 11 | 36 | 3.00 ± 1.73 |
| <i>Steatoda triangulosa</i> 4° | 3 | 31 | 5.40 ± 2.3 |
| <i>Steatoda paykulliana</i> | 13 | 4 | 0.80 ± 0.35 |

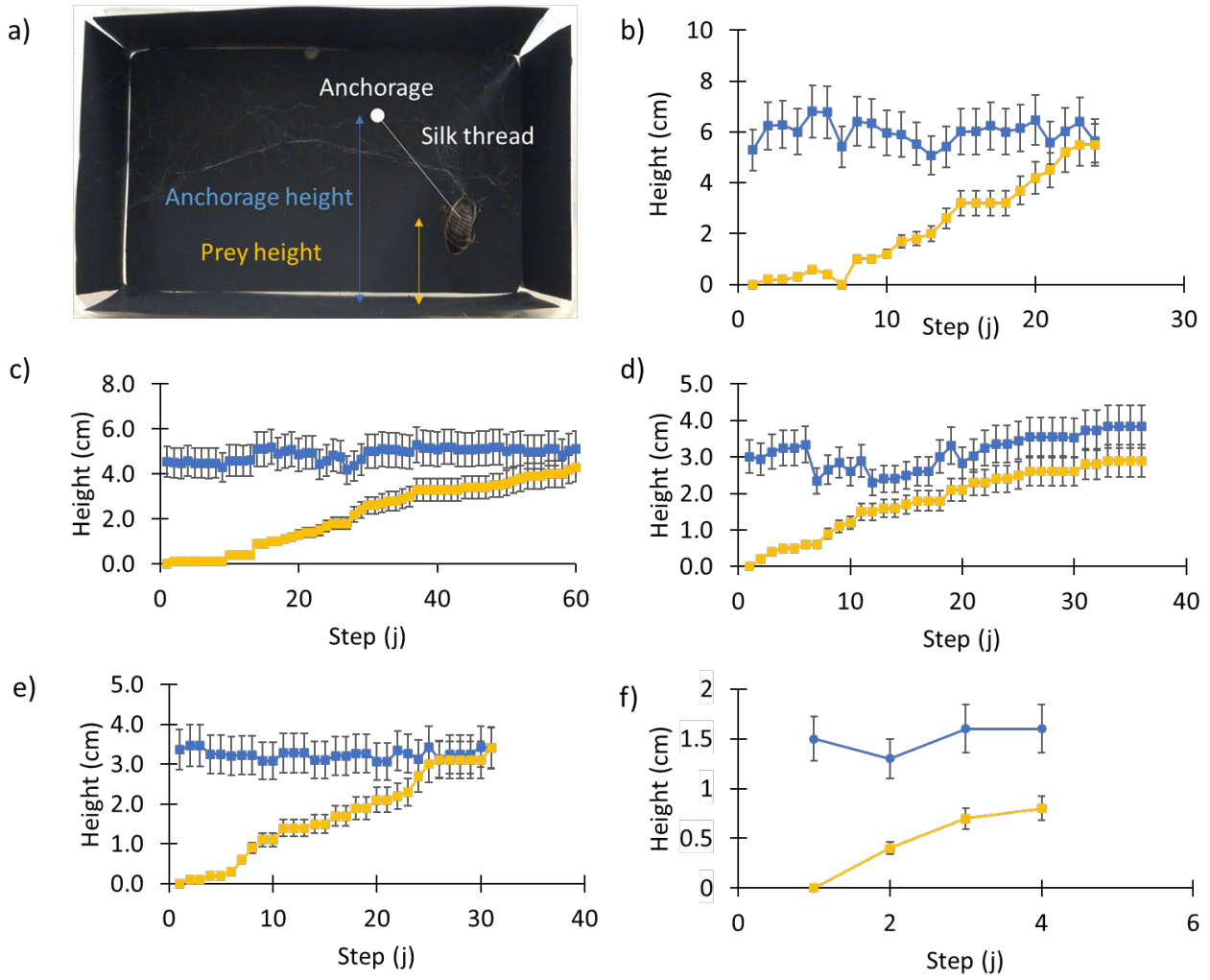
611
 612
 613



614
 615 *Figure S3: a) Length of the inserted threads vs the step of the lifting mechanisms (express in percentage). b) Normalized length of*
 616 *the thread (with respect to the longest) vs the step of the lifting mechanism (expressed in percentage). No particular regularity is*
 617 *observed. The percentage of the process means the state of the hunt with respect to its end (i.e. when the spider stops to spin). It is*
 618 *simply computed by dividing the number of the actual step (i.e. the number of the inserted fibres) for the total number of steps.*

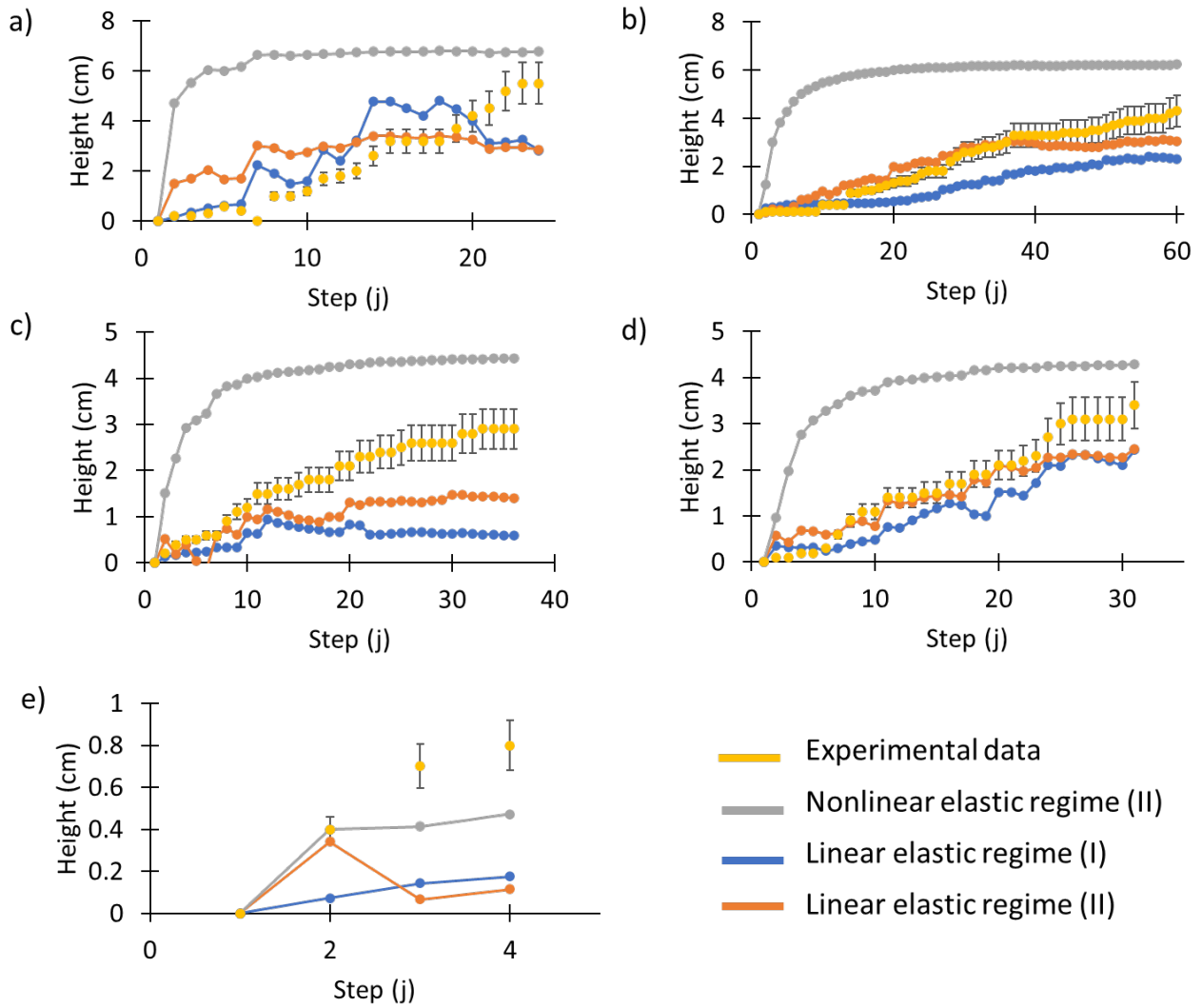


619
 620 *Figure S4: The height profile of the main structure of the tangle webs of the tested spiders.*



621
 622
 623
 624
 625
 626

Figure S5: a) Comparison between the height of the prey and the height of the anchorages during the process. Notice the almost constant height of the anchorages during the predation of the analysed spiders: b) *Steatoda triangulosa* 1°, c) *Steatoda triangulosa* 2°, d) *Steatoda triangulosa* 3°, e) *Steatoda triangulosa* 4° and f) *Steatoda paykulliana*.



627
628
629
630
631
632

Figure S6: Comparison among the theoretical model and the experimental data of the lifting of *Steatoda triangulosa* 1° (a), 2° (b), 3° (c), 4° (d). e) Comparison among the mix-model and the experimental data of the lifting of *Steatoda paykulliana*. Grey lines = nonlinear elastic regime (II strategy); blue lines = linear elastic regime (I strategy); orange line = linear elastic regime (II strategy); yellow points = experimental data.